scientific reports

Check for updates

OPEN

Topological quantum criticality in non-Hermitian extended Kitaev chain

S Rahul[1,2,3] & Sujit Sarkar[1,2]✉

An attempt is made to study the quantum criticality in non-Hermitian system with topological characterization. We use the zero mode solutions to characterize the topological phases and, criticality and also to construct the phase diagram. The Hermitian counterpart of the model Hamiltonian possess quite a few interesting features such as Majorana zero modes (MZMs) at criticality, unique topological phase transition on the critical line and hence these unique features are of an interest to study in the non-Hermitian case also. We observe a unique behavior of critical lines in presence of non-Hermiticity. We study the topological phase transitions in the non-Hermitian case using parametric curves which also reveal the gap closing point through exceptional points. We study bulk and edge properties of the system where at the edge, the stability dependence behavior of MZMs at criticality is studied and at the bulk we study the effect of non-Hermiticity on the topological phases by investigating the behavior of the critical lines. The study of non-Hermiticity on the critical lines revels the rate of receding of the topological phases with respect to the increase in the value of non-Hermiticity. This work gives a new perspective on topological quantum criticality in non-Hermitian quantum system.

From the basic axiom of the quantum physics, we know that observables become self-adjoint operators which are represented by Hermitian matrices[1,2]. These systems have real energy eigenvalues due to their Hermitian properties for example the Schrödinger equation. In general the real physical systems interact with environment depending on the degree of interaction which results in a more complex description[3]. The Effective non-Hermitian (NH) provide an intuitive approach along with wide range of applications. The applications emerge from classical settings such as, optical, electrical systems with effective NH Schrödinger equation to the quantum settings[4,5].

The concepts of non-Hermitian physics found its place in topological states of matter in recent times[4,6]. The introduction of non-Hermiticity altered the concepts of topological systems greatly. The excitation spectrum is no longer real, the definitions of gap in the energy dispersion and the Brillouin zone are completely different when compared to its definitions in Hermitian setting. Features that emerge as a consequence of introduction of non-Hermiticity to the topological systems are complex energy dispersion, EP and modified bulk boundary correspondence[5,7–9]. Complex energy dispersion shows that gap closing and and also the concept of gap is different in non-Hermitian systems. To observe the gap closing behavior the absolute value of the energy spectrum is considered otherwise observing only the real part or imaginary part to identify the topological phase transition will be nonphysical.

An important concept for classification of topological systems is the topological invariant number[10]. For Hermitian systems it is discussed in the above subsections. For non-Hermitian systems, since the curvature function is complex in nature and also the concept of periodic Brillouin zone boundary is altered[11–13]. Hence the regular definition of topological invariant number is not enough in the non-Hermitian setting.

The study of Non-Hermitian systems have gained an immense attention and importance in the recent times when it entered the area of topological systems[6,14–16] but the criticality in non-Hermitian systems is as interesting as compared to its Hermitian counterpart because of the presence of EP[17,18]. These are the points at which the complex eigenvalues become degenerate and also since it is complex in nature, they come in pairs. The interesting properties of the EP are widely observed in experiments . For the topological systems, the EP have been classified as rings and surfaces[18–21].

Non-Hermitian system offers a look into a more realistic and interactive setup, in other words, the non-Hermiticity is the interaction of environment with the system or vice versa. *PT* symmetric Hamiltonians are

[1]Department of Theoretical Sciences, Poornaprajna Institute of Scientific Research, 4, Sadashivanagar, Bangalore 560080, India. [2]Department of Theoretical Sciences, Poornaprajna Institute of Scientific Research, Bidalur Post, Devanhalli, Bangalore Rural 562110, India. [3]Graduate Studies, Manipal Academy of Higher Education, Madhava Nagar, Manipal 576104, India. ✉email: sujit.tifr@gmail.com

non-Hermitian systems, where these Hamiltonians possess real eigenvalues in the *PT* unbroken phase[4,6,20,22,23]. These *PT* symmetric Hamiltonians are widely used in the field of optics because, controlled dissipation can be achieved in these systems[9,24–30].

There have been studies on the non-Hermitian Kitaev system hosting MZMs[31–33]. Topological properties and topological invariant number of non-Hermitian system[11,34–38] are studied where they show stable topological phases and fractional topological invariant number. Many of such non-Hermitian systems show the topological nature and fall under different symmetry classes[39]. There have been tremendous advances in the experimental realizations of non-Hermitian systems in the field of laser physics, acoustics and in the quantum computation[40–45].

Motivation

The definitive clarity of physics for Kitaev chain[46] in presence of non-Hermiticity is understood but the extended Kitaev model (Hermitian) hosts more than one topological phases which is in a way responsible for the appearance of MZMs at criticality. It consists of non-high symmetry critical line where the curvature function diverges at different k values whereas in all other critical lines the excitation the curvature function diverges onnly at a specific k value.

It also possesses multicritical point in which one of them is responsible for the topological phase transition on the critical line to occur. But when it comes to non-Hermitian systems, the excitation spectrum is complex and as a consequence the criticality also changes. Gap closing points are associated with the appearance of EP at which the eigenstates coalesce. Exploration of EP and the effect of γ on the EP are important aspects of non-Hermitian systems. The questions on the topological properties like, how does the concept of criticality change? Since it is complex in nature, how does real and imaginary components behave? Does robustness of the MZMs change with respect to γ? With these important questions, we attempt to answer it by investigating the effects of non-Hermiticity on the extended Kitaev model and its topological phases and criticality.

Model Hamiltonian

We consider an extended Kitaev chain in presence of non-Hermiticity as follows,

$$\begin{aligned} H = &- \lambda_1 \sum_{i=1}^{N-1} (c_i^\dagger c_{i+1} + c_i^\dagger c_{i+1}^\dagger + h.c) - \lambda_2 \sum_{i=1}^{N-1} (c_{i-1}^\dagger c_{i+1} \\ &+ c_{i+1} c_{i-1} + h.c) - (\mu + i\gamma) \sum_{i=1}^{N} (1 - 2c_i^\dagger c_i). \end{aligned} \tag{1}$$

Where λ_1, λ_2, μ and γ corresponds to nearest, next nearest neighbor coupling, chemical potential and non-Hermitian factor respectively.

The Hermitian counterpart of this Hamiltonian has been studied explicitly in the references[47–51] which holds many interesting results such as MZMs at criticality, topological phase transition on the critical line, unique properties of the multicritical points. At the excitation spectra, $E_k = 0$, signaling quantum phase transition there exist three such points of this model in the momentum space are at, $k = 0$, $k = \pm\pi$ and $k = \cos^{-1}(-\frac{\lambda_1}{2\lambda_2})$ giving rise to three critical lines $\lambda_2 = \mu - \lambda_1$, $\lambda_2 = \mu + \lambda_1$ and $\lambda_2 = -\mu$ respectively.

After the Fourier transformation, the Hamiltonian (Eq. 1) becomes,

$$H = \sum_k (2(\mu + i\gamma) - 2\lambda_1 \cos k - 2\lambda_2 \cos 2k) c_k^\dagger c_k + i \sum_k (2\lambda_1 \sin k c_k^\dagger c_{-k}^\dagger + 2\lambda_2 \sin 2k c_k^\dagger c_{-k}^\dagger + h.c). \tag{2}$$

The Hamiltonian written in terms of Anderson pseudo spin form is given by[49,52],

$$H_k = \chi_z(k)\sigma_z - \chi_y(k)\sigma_y = \begin{pmatrix} \chi_z(k) & i\chi_y(k) \\ -i\chi_y(k) & -\chi_z(k) \end{pmatrix}, \tag{3}$$

where $\chi_z(k) = -2\lambda_1 \cos k - 2\lambda_2 \cos 2k + 2(\mu + i\gamma)$, and $\chi_y(k) = 2\lambda_1 \sin k + 2\lambda_2 \sin 2k$ are the components of the Hamiltonian.

Energy dispersion relation is,

$$E_k = \pm\sqrt{(\chi_z(k))^2 + (\chi_y(k))^2}. \tag{4}$$

Generally for the Hermitian case, the topological invariant number W is calculated with the components of Hamiltonian $\chi_z(k)$ and $\chi_y(k)$, i.e.,

$$W = \frac{1}{2\pi} \oint \frac{\partial\theta}{\partial k} dk, \tag{5}$$

where $\theta = \arctan\left(\frac{\chi_y(k)}{\chi_z(k)}\right)$. For the non-Hermitian systems, due to the complex nature of the components of the Hamiltonian the integral definition changes[37].

The energy eigenvalues are complex throughout the parameter space and does not possess any real eigenvalue unlike the *PT* symmetric Hamiltonians[6,53]. Calculating the critical lines becomes tedious for the model Hamiltonian and hence ZMS are used to characterize the topological phases and criticalities.

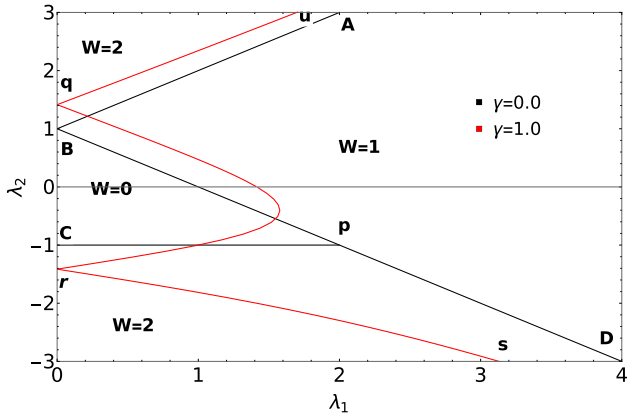

Figure 1. Phase diagram of the model Hamiltonian in presence of γ (= 1.0). Solid black lines corresponds to the topological phase diagram for $\gamma = 0.0$ (Hermitian case).

Results

Zero mode analysis for topological characterization. The introduction of the non-Hermitian factor to the extended Kitaev chain has a significant impact on criticality and topological phase transition. Although all the topological phases remain robust depending on the strength of the non-Hermiticity, a major effect on the criticality is observed. Before we begin the discussion on the effect of γ on the criticality and topological phases, we first brief about the criticality and topological phases in the Hermitian case by understanding the phase diagram. Phase diagram of the Hermitian case is also presented in the Fig. 1 for the sake of comparison with the non-Hermitian case. The Hermitian model consists of three critical lines (solid black line) "AB", "BD" and "Cq" distinguishing topological phases $W = 0, W = 1$ and $W = 2$.

For the Hermitian case, the topological phases are characterized using integral definition of winding number W[47,49,50] whereas for the non-Hermitian model the topological phases are using ZMS. From the Fig. 1, it can be clearly observed that the critical line "Cq" is not present for the non-Hermitian case (critical lines presented in red color).

In the positive λ_2 region of phase diagram Fig. 1, the effect of γ on these critical lines is just a parallel shift. In the negative λ_2 region, the critical line follows the curved path (q to r) as shown in the Fig. 1. The critical line (r to s) also follows a curved path. These critical lines following the curved path for the non-Hermitian case is the consequence of the non-Hermiticity.

Here construct the phase diagram of the non-Hermitian model using the ZMS.

Topological phases for the non-Hermitian case are characterized using ZMS which is presented as follows. Substituting the exponential forms of $\cos k$ and $\sin k$, Eq. (3) becomes,

$$\begin{aligned} H = &\left[2\lambda_1 \frac{1}{2}(e^{-ik} + e^{ik}) + 2\lambda_2 \frac{1}{2}(e^{-2ik} + e^{2ik} + 2(\mu + i\gamma))\right]\sigma_z \\ &+ i\left[2\lambda_1 \frac{1}{2}(e^{ik} - e^{-ik}) + 2\lambda_2 \frac{1}{2}(e^{2ik} - e^{-2ik})\right]\sigma_y. \end{aligned} \tag{6}$$

Solving the Eq. (6) for $H^2 = 0$, we obtain the ZMS as,

$$X_\pm = \frac{-\lambda_1 \pm \sqrt{\lambda_1^2 + 4\lambda_2(\mu + i\gamma)}}{2\lambda_2}. \tag{7}$$

The detailed derivation of ZMS from the model Hamiltonian is relegated in the "Method" Section.

These ZMS (Eq. 7) are nothing but the zeros of a model Hamiltonian that can be written in the form of a complex function[47,54]. Zeros lying inside the unit circle presented in the Fig. 3 indicates topological phase, and zeros lying outside the unit circle represents a non-topological phase whereas zeros lying on the unit circle corresponds to criticality.

In this study, the ZMS are studied as a function of λ_1 to understand the topological phases and phase boundaries. The absolute value of ZMS is considered because the roots are complex in nature.

The ZMS $X_\pm > 1$ corresponds to topologically trivial phase whereas $X_+ > 1$ and $X_+ < 1$ corresponds to the topological phase with winding number $W = 1$. Correspondingly $X_\pm < 1$ represents topological phase with winding number $W = 2$[46].

In the Fig. 2, red and blue curves are the roots representing $W = 0$ to $W = 1$ transition and magenta and black curves are the roots representing $W = 1$ to $W = 2$ transition. To specify the transition point using ZMS, parallel to the λ_1 axis, a reference line (unit line), $y = 1$ is drawn which acts in a same way as that of the unit circle drawn to analyze the zeros of a complex function. The point of the intersection between one of the ZMS and the unit line marks the transition point which is represented in blue dots ($p1$ and $p2$) in the Fig. 2.

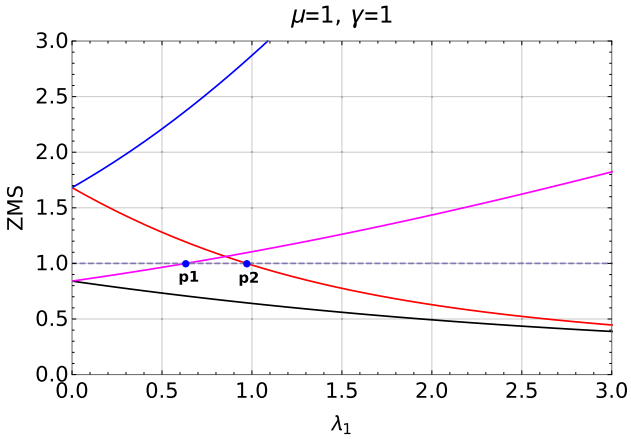

Figure 2. Zero mode solutions plotted with respect to the parameter λ_1 shows both $W = 0$ to $W = 1(\lambda_2 = 0.5)$ and $W = 1$ to $W = 2\,(\lambda_2 = 2.0)$ topological phase transitions. The red dot (p1 and p2) represent the transition points. The ZMS, X_+ (red) and X_- (blue) are plotted in y-axis.

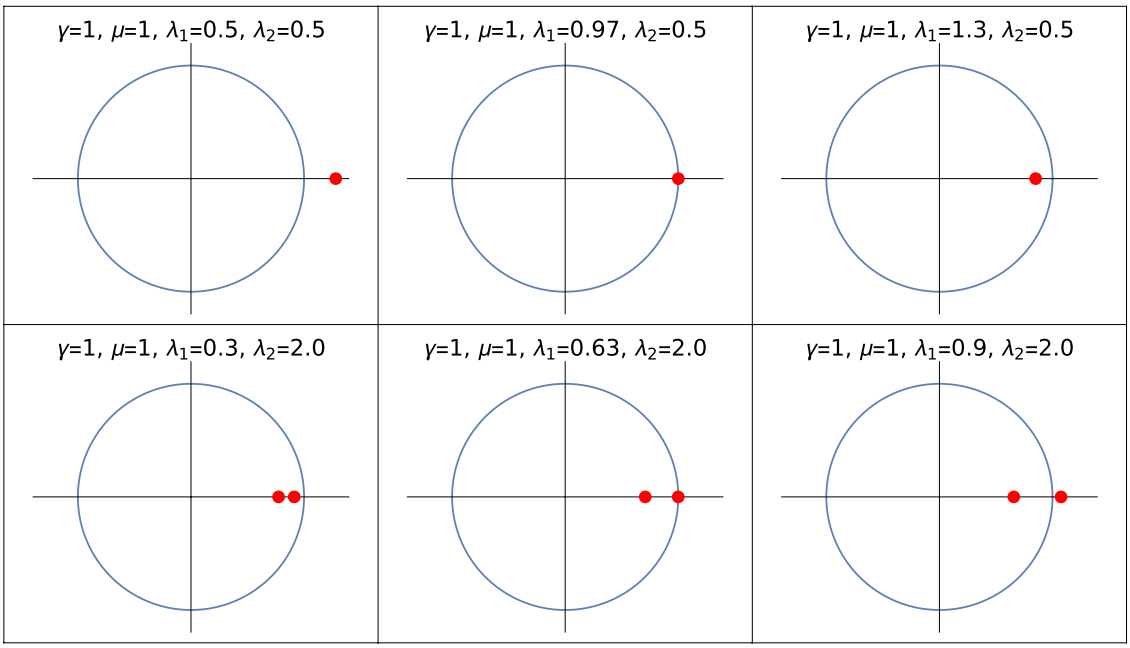

Figure 3. Zeros of a Hamiltonian plotted with respect to a unit circle for the transitions, $W = 0$ to $W = 1$ $(\lambda_2 = 0.5)$ (upper panel) and $W = 1$ to $W = 2\,(\lambda_2 = 2.0)$ (lower panel). Two red dots corresponds to the zeros.

Value of the roots greater than 1 corresponds to the non-topological phase whereas less than 1 corresponds to topological phase. Transition points $p1$ and $p2$ marks the transitions between $W = 2$ to 1 and $W = 0$ to 1 respectively with fixed positive value of λ_2 ($\lambda_2 = 0.5, 2.0$). Keeping track of these transition points via the ZMS method provides the phase diagram of the model Hamiltonian (Fig. 1). The transitions through the curved critical lines in the negative λ_2 region are analyzed in the further sections.

In the Fig. 3 we can see the ZMS plotted with respected to a unit circle whereas the unit circle is made into a unit line in the Fig. 2. The zeros falling inside the unit circle corresponds to the topologically non-trivial phase whereas the zeros falling on the unit circle and outside the unit circle corresponds to the transition and topologically trivial phase respectively. In both Figs. 2 and 3 the same zeros are plotted with respect to a system parameter λ_1 and a unit circle respectively.

Parametric curves and exceptional points. In the Hermitian systems, the topological phase transition is seen when the parametric curve touches the origin. When the parametric encloses the origin, it corresponds to topological phase[50]. Similarly, in the case of non-Hermitian systems, the topological phase is represented when the parametric curves enclose the EP whereas the transition is marked when it touches EP when the system is going from one topological phase to another. At EP the eigenstates of corresponding complex eigenvalues coalesce becoming degenerate and also at these points the Hamiltonian is nondiagonalizable[17,55]. These EP are

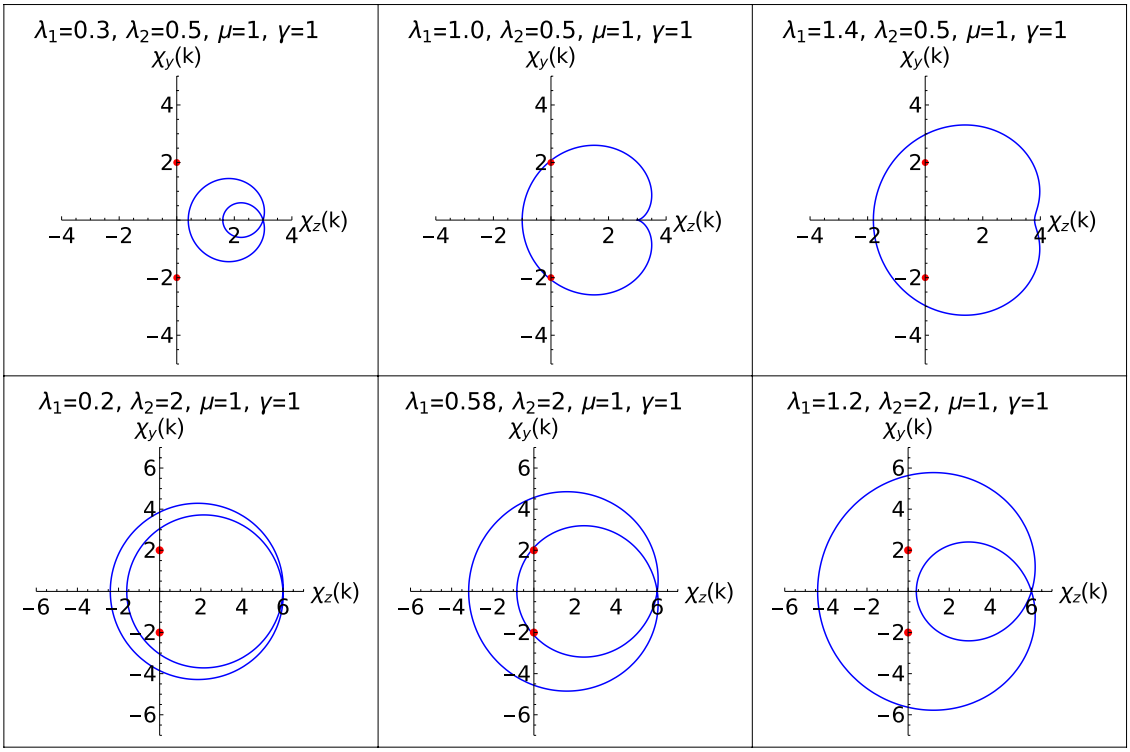

Figure 4. Parametric plots are represent the topological phase transitions in the positive λ_2 region. Upper and lower panel corresponds to W=1 and $W = 2$ to 1 respectively. Middle plot in both the panels represents the parametric curves at critical points.

special kind of degenerate points at which the excitation energy becomes zero, i.e., at $h_x^2 + h_y^2 = 0$. The positions of EP are given as,

$$h_{xr} = -h_{yi}, \quad \text{and} \quad h_{yr} = h_{xi} \text{or} h_{xr} = h_{yi}, \quad \text{and} \quad h_{yr} = -h_{xi}. \tag{8}$$

Where h_{yr}, h_{yi}, h_{xr} and h_{xi} are the real and imaginary parts of components h_y and h_x of the model Hamiltonian (The detailed derivation is relegated to the "Method" Section). Depending on the value of the non-Hermitian factor γ, the positions of the EP change along the χ_y axis.

The parametric curves for topological phase transitions, W=0–1 and $W = 2$ to 1 are studied in the Fig. 4. Two red spots on the χ_y axis at 2,-2 shown in the Fig. 4 are the positions of EP through which the transition occurs. In the positive λ_2 region, the critical lines remain linear in presence of the non-Hermiticity. We observe a parallel shift in the critical lines for increase in the value of γ. Positive λ_2 region offers two topological phase transition, W=0–1 and W=2 to 1.

In the upper panel of the Fig. 4, gapped phase $W = 0$ (left plot), transition point (middle plot) and gapped phase $W = 1$ (right plot) are shown.

Similarly in the lower panel, transition from $W = 2$ to 1 is depicted. As seen from the phase diagram, Fig. 1, critical lines in the negative λ_2 region behave in a different manner where it is no longer linear or follows a parallel shift when compared to the critical lines in positive λ_2 region. In order to understand the topological phase transitions in the negative λ_2 region, the parametric curves are plotted to depict the transition between gapped phases as shown in the Figs. 5 and 6.

The deflection of the critical line "qr" as shown in the phase diagram Fig. 1 is a novel behavior observed in the non-Hermitian system. Figure 5 shows the transition between W=0–1. Similarly, parametric plot representing W=1–2 for two different values of λ_1 is also shown in the Fig. 6.

In the Fig. 6, we present the topological phase transition between $W = 1$ and 2 for two different values of λ_1. Upper panel is for $\lambda_1 = 0.4$ where left plot corresponds to $W = 1$ phase, middle plot corresponds the transition and the right plot corresponds to topological phase $W = 2$.

Parametric curves show, gap closing at the topological phase transition points for two different values of λ_1. Deviated critical lines shown in the phase diagram, Fig. 1, is supported by the parametric curves. Due to this deviation of critical line, the multicritical point is displaced and as a result, the nature of the multicrititcal point is also changed. Observing Figs. 4, 5 and 6, they clearly show that the parametric curve encloses the EP which corresponds to topologically non-trivial phase and similarly it does not enclose the EP which corresponds to topologically trivial phase. With Changed nature of criticality also the parametric curves presents a simple form to characterize the topological phases.

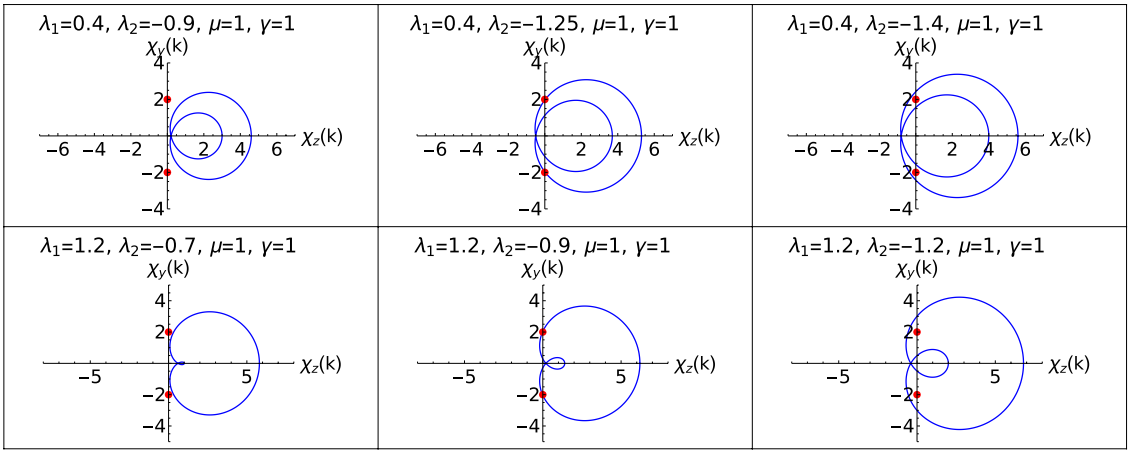

Figure 5. Parametric plots representing the topological phase transitions in the negative λ_2 region. Upper and lower panel corresponds to W=0–1 for different values of λ_1 respectively. Middle plot in both the panels represents the parametric curves at critical points.

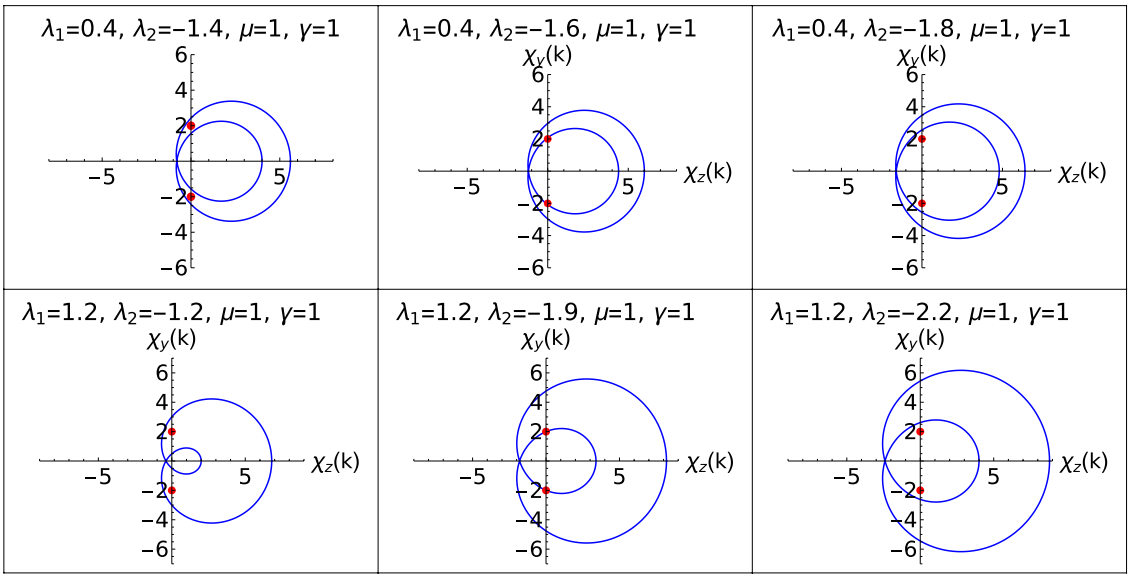

Figure 6. Parametric plots representing the topological phase transitions in the negative λ_2 region. Upper and lower panel corresponds to W=1–2 for different values of λ_1 respectively. Middle plot in both the panels represents the parametric curves at critical points.

Bulk edge properties at quantum criticality

In this section, we study the concept of bulk edge properties for the model in presence of γ. In the topological systems, the concept of bulk-boundary correspondence holds together the bulk and edge properties which establishes a robust relation between them. In Hermitian case, the validation of bulk and edge properties for the gapped phases is well established[56], and since the MZMs appear at the criticality too, the validation of bulk-boundary correspondence at criticality is also observed[47]. The scenario of bulk-boundary correspondence in non-Hermitian case entirely different when compared to the Hermitian case. Although the breakdown of conventional bulk-boundary correspondence in the non-Hermitian systems has been reported[57,58], there has been attempt to build a generalized bulk-boundary correspondence in the recent years[59–62]. We study both, edge property i.e., the robustness of MZMs at criticality and bulk property i.e., the effect of γ on topological phases.

Majorana zero modes at criticality. Here in this section we study the effect of non-Hermiticity γ over the criticalities and MZMs present at the criticality. For the non-Hermitian model Hamiltonian considered, MZMs are present in their respective topological phases just as in the case of Hermitian systems. Authors of Ref.[47] have studied the characterization and MZMs at criticality and similarly in the non-Hermitian systems, we observe the MZMs at criticality. Criticality hosts MZMs when it separates topological phases with winding number $W > 0$.

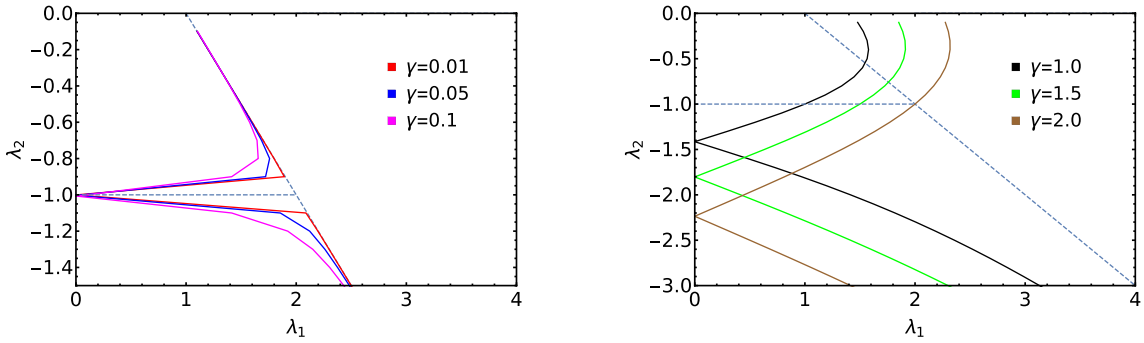

Figure 7. Phase diagram of λ_2 with λ_1. All the intersecting points on the negative λ_2 axis in the right plot are the positions of multicritical point for different values of γ.

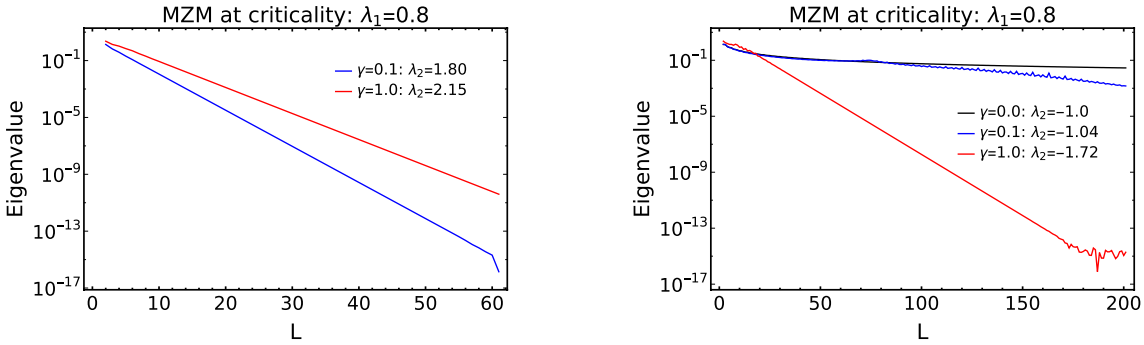

Figure 8. Behavior of zero mode eigenvalues at criticality "qu" and "rs" (refer to the Fig. 1) with system size for different values of γ.

For example, critical lines separating $W = 1$ and $W = 2$ and higher order winding number hosts MZMs which is dependent on the difference between the winding number of two topological phases.

In the non-Hermitian system under consideration, critical lines, "qu" and "rs", shown in the phase diagram, Fig. 1, hosts the MZMs because they separate topological phases $W = 2$ and $W = 1$. In the Hermitian counterpart of the model Hamiltonian, it has three critical lines where one of them is present in the negative λ_2 region which separates $W = 0$ and $W = 2$ topological phases. But with the introduction of the non-Hermitian factor γ, the the critical line that separates $W = 0$ and 2 topological phases no longer exist which can be seen from the Fig. 7. The phase between the critical line "qu" and "rs" is acquired by a topological phase $W = 1$. Hence with the introduction of γ induces a successive topological phase transition between the $W = 0, W = 1$ and $W = 2$. Whereas in the Hermitian case ($\gamma = 0$) it was only a topological phase transitions between $W = 0$ and $W = 2$. Due to the appearance of topological phase $W = 1$ in between the critical lines "qu" and "rs", the critical line "rs" hosts MZMs at criticality.

The acquirement of the topological phase $W = 1$ can be clearly seen from the Fig. 7 where for lesser γ values which is represented in the left plot, the acquired area is less and as the value of γ is increased the acquired area is more as seen from the right plot.

Since the critical lines "qu" and "rs" host MZMs, the stability of these MZMs are studied in the Fig. 8. For the critical line "qu", the zero mode eigenvalues decay exponentially for different values of γ. For the critical line "rs", the situation is a bit different because if γ tends to zero, the critical line of the Hermitian Hamiltonian does not host the MZMs at criticality which can be see from the right plot (black line) of Fig. 8. As the values of γ, the critical line "rs" hosts MZMs because for finite γ value it separates $W = 1$ and $W = 2$ topological phases. Hence the MZMs localize at the criticality "rs" for larger system size when compared to the localization of MZMs at the criticality "qu" which can be seen from the Fig. 8.

With higher values of γ, the MZMs on the critical line "rs" becomes more robust because the acquired area by the topological phase $W = 1$ is more. The acquirement by the topological phase $W = 1$ is caused by the displacement of the multicritical point from its previous position $\lambda_2 = -1$ and $\lambda_1 = 2.0$ (Hermitian case) to its new position $\lambda_2 = \sqrt{\mu^2 + \gamma^2}$ and $\lambda_1 = 0$ (non-Hermitian case).

Effect of non-Hermiticity on the topological phases and criticality. Here in this section we extend the study of effect of non-Hermiticity γ over the criticalities using the quantity which measures the variation of the difference of the critical lines with changing γ.

In the Hermitian case, extended Kitaev chain possess three gapped topological phases and respectively three critical lines. The additional feature of the Hermitian extended Kitaev chain is the presence of multicritical point at $\lambda_1 = 2$ and $\lambda_2 = -1$ which has been extensively studied in reference[47,48]. From the ZMS the new critical lines

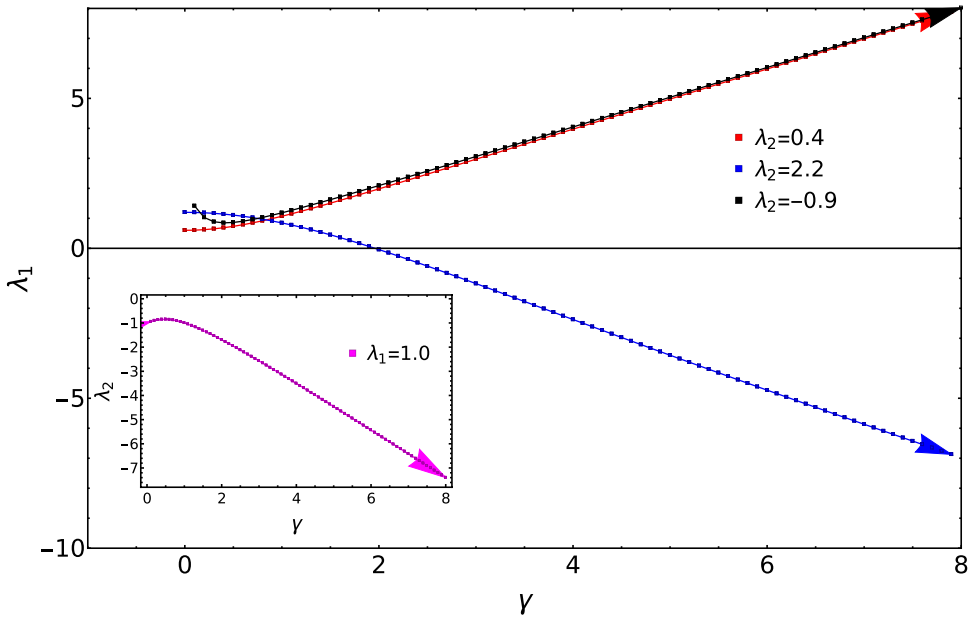

Figure 9. Behavior of critical lines with γ for different values of λ_1 and λ_2. Inset represents the behavior of critical line with λ_2.

were identified and the phase diagram is constructed (Fig. 1). As presented in the Fig. 7, the positions of the critical lines change for different values of γ.

Considering topological phase transition between all the topological phases, the critical lines move as shown in the Fig. 9. In the Fig. 9, we present the movement of critical lines with respect to γ for fixed values of λ_1 and λ_2.

Red, black and blue curves of Fig. 9 are respectively for $\lambda_2 = 0.4, 2.2$ and -0.9 representing topological phase transitions $w = 0$ to 1, $W = 1$ to 2 and $W = 0$ to 1. It reveals from this study that for $W = 0$ to 1 transition in the negative λ_2 region the critical points does not continuously increase with respect to γ like the red curve, instead they decrease initially and then increase with respect to the increase in the value of γ.

This happens because, critical point for $\lambda_2 = -0.9$ move backwards first and then moves forward towards higher values of λ_1. For $W = 0$ to 1 and $W = 2$ to 1 topological phase transitions, the backward movement of the critical line is not observed.

The arrow mark shows the direction of the movement of the critical lines. Blue curve corresponding to $W = 2$ to 1 decreases and moves eventually to the negative λ_1 plain because, as the value of γ is increased, the critical line for $\lambda_2 = 2.2$ moves backward and eventually goes to negative λ_1 plain because the same critical line is continued in the negative λ_1 plain. Both red and blue curves show increase and decrease respectively unlike the black curve.

Inset of the Fig. 9 corresponds to the critical lines plotted with respect to γ for fixed value of $\lambda_1 = 1.0$. This represent the transition from $W = 1$ to 2 topological phases in negative λ_2 regime. Even in this phase transition, there is a slight increase in the values of critical points and as the value of γ is increased, the value of the critical points decrease continuously. This is also because of the backward movement for certain value of γ and the forward movement for the rest of the values of γ.

Studying the movement and the direction of the critical points with respect to γ for all the transitions, the rate of receding in both positive and negative direction with respect to γ is also studied which is presented in the Fig. 10.

The difference between the values of the critical points represented as $x_{n+1} - x_n$ is calculated and it is plotted with respect to the γ. The quantity $x_{n+1} - x_n$ corresponds to the difference of the critical lines with respect to different values of γ starting from $\gamma = 1$ to 8. The quantity $x_{n+1} - x_n$ signifying the rate of receding of critical points with respect to γ reveals some interesting behavior in the Fig. 10. Plots (a) and (b) of the Fig. 10 in the upper panel corresponds to the values of $\lambda_2 = 0.4$ and 2.2. These values represent the transition from $W = 0$ to 1 and $W = 2$ to 1 topological phases.

In the plot (a) of the Fig.10, the difference, $x_{n+1} - x_n$ rises sharply and saturates at 1 signifying that spacing between the critical points increases rapidly till $\gamma = 2$ and for $\gamma > 2$, the spacing remains constant which is depicted by the saturation of the curve. The quantity, $x_{n+1} - x_n$ is negative in the plot (b) signifying only the backward movement of critical points with respect to γ and it does not mean that spacing between the critical points are negative.

Plot (b) of Fig. 10 corresponds to $W = 2$ to 1 topological phase transition and as the plot shows, the difference becomes large with increasing γ value but in the opposite direction. Critical points show an interesting behavior in the negative quadrant of λ_2 (plot (c) and (d) of Fig. 10) where they show both and forward movement with respect to increase in the values of γ. Due to the modification of critical lines where they are no longer linear and also with he displacement of multicritical point, they show the corresponding behavior (refer Fig. 10) for increasing values of γ. This analysis shows a detailed effects of γ on the topological phases and criticality.

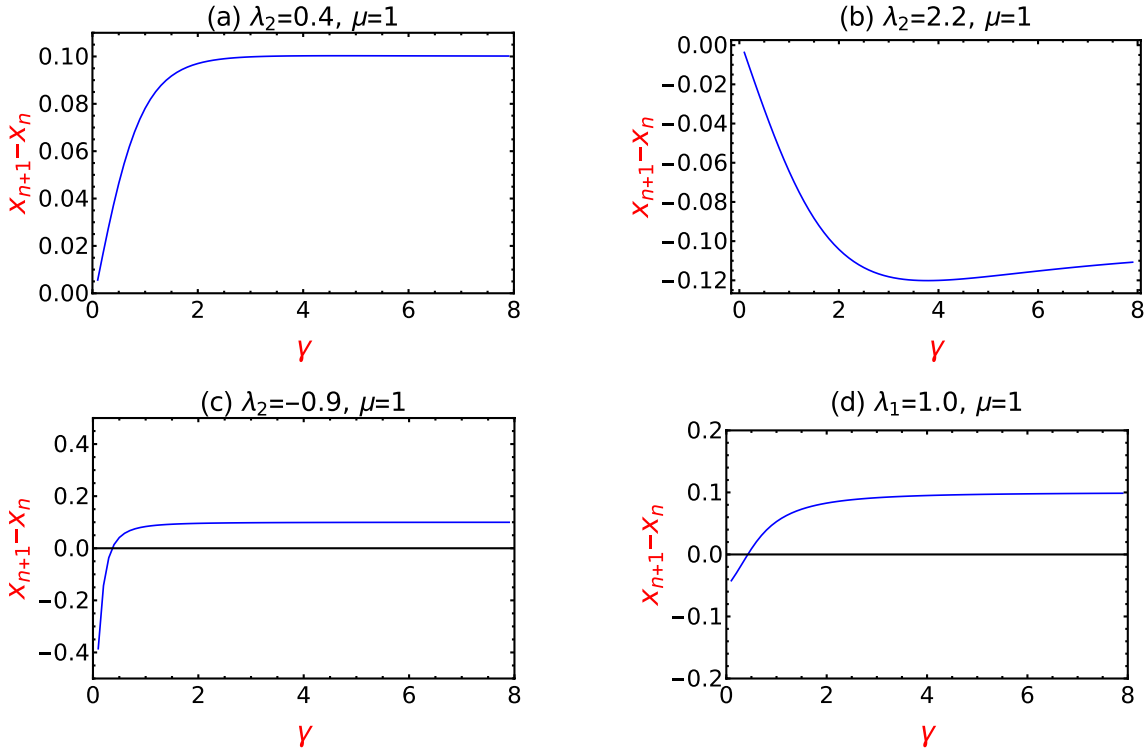

Figure 10. Variations in the difference of critical lines $(x_{n+1} - x_n)$ with γ for fixed values of λ_1 and λ_2.

Discussion

We have computed the critical lines of non-Hermitian extended Kitaev chain by using an elegant method of zero mode solutions. We have investigated and observed an interesting phenomenon where the critical lines are modified. It also shows the disappearance of multicritical point from its usual location. Parametric curve study has been performed in order to validate the nature of the critical lines. The topological characterization studied using parametric curves results in calculating the EP and its dependence on the non-Hermitian factor. We also have investigated the MZMs at criticality and its stability. We have observed a displacement in the multicritical point position due to non-Hermitian factor γ. Finally the effect of γ on the topological phases has studied by calculating the difference of the positions of critical lines for different values of γ. This shows the rate at which the critical lines recede. Critical points for corresponding values of γ have been calculated and its difference has studied. This showed the rate of receding which gives the dynamics of critical lines for increasing values of γ.

Methods

Zero mode solutions. The model Hamiltonian can be written as,

$$H_k = \chi_z(k)\sigma_z + \chi_y(k)\sigma_y, \tag{9}$$

where $\chi_z(k) = 2\lambda_1 \cos k + 2\lambda_2 \cos 2k - 2(\mu + i\gamma)$, and $\chi_y(k) = 2\lambda_1 \sin k + 2\lambda_2 \sin 2k$.

Substituting the exponential forms of $\cos k$ and $\sin k$, Eq. (9) becomes,

$$\begin{aligned} H = &\left[2\lambda_1 \frac{1}{2}(e^{-ik} + e^{ik}) + 2\lambda_2 \frac{1}{2}(e^{-2ik} + e^{2ik} + 2(\mu + i\gamma))\right]\sigma_z \\ &+ i\left[2\lambda_1 \frac{1}{2}(e^{ik} - e^{-ik}) + 2\lambda_2 \frac{1}{2}(e^{2ik} - e^{-2ik})\right]\sigma_y. \end{aligned} \tag{10}$$

We replace $e^{-ik} = e^q$, Eq. (10) becomes,

$$\begin{aligned} H = &\left[2\lambda_1 \frac{1}{2}(e^{q} + e^{-q}) + 2\lambda_2 \frac{1}{2}(e^{2q} + e^{-2q}) + 2(\mu + i\gamma)\right]\sigma_z \\ &+ i\left[2\lambda_1 \frac{1}{2}(e^{-q} - e^{q}) + 2\lambda_2 \frac{1}{2}(e^{-2q} - e^{2q})\right]\sigma_y. \end{aligned} \tag{11}$$

To find the zero mode solutions, we make $H^2 = 0$. By solving the Eq. (11), we get,

$$2\lambda_1 \cosh q + 2\lambda_2 \cosh 2q - 2(\mu + i\gamma) = \pm 2\lambda_1 \sinh q + 2\lambda_2 \sinh 2q. \tag{12}$$

Equation 12 shows that there will be more than one solution. Considering the Eq. (11) and squaring both sides with $H = 0$, we get,

$$\left(2\lambda_1 \cosh q + 2\lambda_2 \cosh 2q - 2(\mu + i\gamma)\right) + i\left(2\lambda_1 \sinh q + 2\lambda_2 \sinh 2q\right) = 0. \tag{13}$$

Substituting back the exponential forms to the respective terms, we get,

$$\begin{aligned}&\left[2\lambda_1 \frac{1}{2}(e^q + e^{-q}) + 2\lambda_2 \frac{1}{2}(e^{2q} + e^{-2q} + 2(\mu + i\gamma))\right] \\ &+ \left[2\lambda_1 \frac{1}{2}(e^{-q} - e^q) + 2\lambda_2 \frac{1}{2}(e^{-2q} - e^{2q})\right] = 0\end{aligned} \tag{14}$$

Simplifying the Eq. (14), we end up with a quadratic equation,

$$2\lambda_1 \frac{1}{2}e^q + 2\lambda_2 \frac{1}{2}e^{2q} + 2(\mu + i\gamma) + 2\lambda_1 \frac{1}{2}e^q + 2\lambda_2 \frac{1}{2}e^{2q} = 0. \tag{15}$$

Simplifying the Eq. (15) to a quadratic form and substituting $e^q = X$,

$$\lambda_2 X^2 + \lambda_1 X + (\mu + i\gamma) = 0. \tag{16}$$

The roots of this quadratic Equation is given by,

$$X = \frac{-\lambda_1 \pm \sqrt{\lambda_1^2 + 4\lambda_2(\mu + i\gamma)}}{2\lambda_2} \tag{17}$$

The roots Eq. (17) are the solutions of zero modes.

Exceptional points. Exceptional points arise naturally in the non-Hermitian systems because of the complex nature of the system. In the Hermitian systems, the singularity or the critical points are obtained in a straight forward manner. In non-Hermitian systems, specially in the *PT* symmetric Hamiltonians, obtaining gap closing points or the so called exceptional points is a bit tricky.

For example, considering a 2×2 Hamiltonian,

$$\begin{pmatrix} i\gamma & -J \\ -J & -i\gamma \end{pmatrix}, \tag{18}$$

where J and γ are non negative numbers.

The energy eigenvalues are given by,

$$E = \pm\sqrt{J^2 - \gamma^2}. \tag{19}$$

From the Eq. (19), one can see that the eigenvalues are real when $J > \gamma$ which marks the *PT* unbroken region. For $J < \gamma$, the eigenvalues are all complex which marks the *PT* broken region. For $J = \gamma$ is the transition point between the *PT* unbroken and broken phases.

Since exceptional points arises naturally irrespective of systems obeying *PT* symmetry, model Hamiltonian under consideration also possess exceptional points.

Exceptional points for such systems can be seen from an example.

Consider a 2×2 Hamiltonian,

$$\begin{pmatrix} h_z(k) + i\gamma & h_y(k) \\ -h_y(k) & -(h_z(k) + i\gamma) \end{pmatrix}, \tag{20}$$

where h_y and h_z are the components of the Hamiltonian.

The eigenvalues are given by,

$$E = \pm\sqrt{(h_y)^2 + (h_z + i\gamma)^2}. \tag{21}$$

To find the exceptional points is nothing but finding the condition when $|E| = 0$. Hence, $|E|$ will become zero, when $h_z = 0$ and $h_y = \pm\gamma$. The condition $h_y = \pm\gamma$ gives the location of the exceptional points.

Received: 18 November 2021; Accepted: 11 April 2022
Published online: 28 April 2022

References

1. Messiah, A. *Quantum Mechanics*. In No. v. 2 in Dover books on physics (Dover Publications, 2014) https://books.google.co.in/books?id=8FvLAgAAQBAJ.
2. Griffiths, D. J. & Schroeter, D. F. *Introduction to Quantum Mechanics* 3rd edn. (Cambridge University Press, 2018).
3. Moiseyev, N. *Non-Hermitian Quantum Mechanics* (Cambridge University Press, 2011).
4. Bender, C. M. Making sense of non-hermitian hamiltonians. *Rep. Prog. Phys.* **70**, 947 (2007).

5. Bergholtz, E. J., Budich, J. C. & Kunst, F. K. Exceptional topology of non-hermitian systems. arXiv preprint arXiv:1912.10048 (2019).
6. Bender, C. M. & Boettcher, S. Real spectra in non-hermitian hamiltonians having p t symmetry. *Phys. Rev. Lett.* **80**, 5243 (1998).
7. Shen, H., Zhen, B. & Fu, L. Topological band theory for non-hermitian hamiltonians. *Phys. Rev. Lett.* **120**, 146402 (2018).
8. Kunst, F. K., Edvardsson, E., Budich, J. C. & Bergholtz, E. J. Biorthogonal bulk-boundary correspondence in non-hermitian systems. *Phys. Rev. Lett.* **121**, 026808 (2018).
9. Ashida, Y., Gong, Z. & Ueda, M. Non-hermitian physics. *Adv. Phys.* **69**, 249–435 (2020).
10. Fu, L. & Kane, C. L. Superconducting proximity effect and majorana fermions at the surface of a topological insulator. *Phys. Rev. Lett.* **100**, 096407 (2008).
11. Yao, S. & Wang, Z. Edge states and topological invariants of non-hermitian systems. *Phys. Rev. Lett.* **121**, 086803 (2018).
12. Lee, J. Y., Ahn, J., Zhou, H. & Vishwanath, A. Topological correspondence between hermitian and non-hermitian systems: anomalous dynamics. *Phys. Rev. Lett.* **123**, 206404 (2019).
13. Ghatak, A. & Das, T. New topological invariants in non-hermitian systems. *J. Phys. Condens. Matter* **31**, 263001 (2019).
14. Leykam, D., Bliokh, K. Y., Huang, C., Chong, Y. D. & Nori, F. Edge modes, degeneracies, and topological numbers in non-hermitian systems. *Phys. Rev. Lett.* **118**, 040401 (2017).
15. Bender, C., Fring, A., Günther, U. & Jones, H. Quantum physics with non-hermitian operators. *J. Phys. A Math. Theor.* **45**, 440301 (2012).
16. Yamamoto, K., Nakagawa, M., Tezuka, M., Ueda, M. & Kawakami, N. Universal properties of dissipative tomonaga-luttinger liquids: A case study of a non-hermitian xxz spin chain. arXiv preprint arXiv:2112.12467 (2021).
17. Heiss, W. The physics of exceptional points. *J. Phys. A Math. Theor.* **45**, 444016 (2012).
18. Heiss, D. Circling exceptional points. *Nature Phys.* **12**, 823–824 (2016).
19. Okugawa, R. & Yokoyama, T. Topological exceptional surfaces in non-hermitian systems with parity-time and parity-particle-hole symmetries. *Phys. Rev. B* **99**, 041202 (2019).
20. Kawabata, K., Bessho, T. & Sato, M. Classification of exceptional points and non-hermitian topological semimetals. *Phys. Rev. Lett.* **123**, 066405 (2019).
21. Yoshida, T., Peters, R., Kawakami, N. & Hatsugai, Y. Symmetry-protected exceptional rings in two-dimensional correlated systems with chiral symmetry. *Phys. Rev. B* **99**, 121101 (2019).
22. Chiu, C.-K., Teo, J. C., Schnyder, A. P. & Ryu, S. Classification of topological quantum matter with symmetries. *Rev. Mod. Phys.* **88**, 035005 (2016).
23. Bender, C. M. *PT Symmetry: In Quantum and Classical Physics* (World Scientific, 2019).
24. Rüter, C. E. *et al.* Observation of parity-time symmetry in optics. *Nature Phys.* **6**, 192–195 (2010).
25. Kawabata, K., Ashida, Y., Katsura, H. & Ueda, M. Parity-time-symmetric topological superconductor. *Phys. Rev. B* **98**, 085116 (2018).
26. Peng, B. *et al.* Parity-time-symmetric whispering-gallery microcavities. *Nature Phys.* **10**, 394–398 (2014).
27. Xiao, L. *et al.* Observation of topological edge states in parity-time-symmetric quantum walks. *Nature Phys.* **13**, 1117–1123 (2017).
28. Cai, X. Boundary-dependent self-dualities, winding numbers, and asymmetrical localization in non-hermitian aperiodic one-dimensional models. *Phys. Rev. B* **103**, 014201 (2021).
29. El-Ganainy, R., Khajavikhan, M., Christodoulides, D. N. & Ozdemir, S. K. The dawn of non-hermitian optics. *Commun. Phys.* **2**, 1–5 (2019).
30. El-Ganainy, R. *et al.* Non-hermitian physics and pt symmetry. *Nature Phys.* **14**, 11–19 (2018).
31. Wang, X., Liu, T., Xiong, Y. & Tong, P. Spontaneous pt-symmetry breaking in non-hermitian kitaev and extended kitaev models. *Phys. Rev. A* **92**, 012116 (2015).
32. Zeng, Q.-B., Zhu, B., Chen, S., You, L. & Lü, R. Non-hermitian kitaev chain with complex on-site potentials. *Phys. Rev. A* **94**, 022119 (2016).
33. Esaki, K., Sato, M., Hasebe, K. & Kohmoto, M. Edge states and topological phases in non-hermitian systems. *Phys. Rev. B* **84**, 205128 (2011).
34. Lieu, S. Topological phases in the non-hermitian su-schrieffer-heeger model. *Phys. Rev. B* **97**, 045106 (2018).
35. Zhu, B., Lü, R. & Chen, S. Pt symmetry in the non-hermitian su-schrieffer-heeger model with complex boundary potentials. *Phys. Rev. A* **89**, 062102 (2014).
36. He, Y. & Chien, C.-C. Non-hermitian generalizations of extended su-schrieffer-heeger models. *J. Phys. Condens. Matter* **33**, 085501 (2020).
37. Yin, C., Jiang, H., Li, L., Lü, R. & Chen, S. Geometrical meaning of winding number and its characterization of topological phases in one-dimensional chiral non-hermitian systems. *Phys. Rev. A* **97**, 052115 (2018).
38. Navarro-Labastida, L. A., Domínguez-Serna, F. A. & Rojas, F. Geometrical phases and entanglement in real space for 1d ssh topological insulator: effects of first and second neighbor-hoppings and intra-cell modulation. arXiv preprint arXiv:2106.02756 (2021).
39. Kawabata, K., Shiozaki, K., Ueda, M. & Sato, M. Symmetry and topology in non-hermitian physics. *Phys. Rev. X* **9**, 041015 (2019).
40. Zeuner, J. M. *et al.* Observation of a topological transition in the bulk of a non-hermitian system. *Phys. Rev. Lett.* **115**, 040402 (2015).
41. Ozawa, T. *et al.* Topological photonics. *Rev. Mod. Phys.* **91**, 015006 (2019).
42. Parto, M. *et al.* Edge-mode lasing in 1d topological active arrays. *Phys. Rev. Lett.* **120**, 113901 (2018).
43. Zhang, L.-F. *et al.* Machine learning topological invariants of non-hermitian systems. *Phys. Rev. A* **103**, 012419 (2021).
44. Parto, M., Liu, Y. G., Bahari, B., Khajavikhan, M. & Christodoulides, D. N. Non-hermitian and topological photonics: optics at an exceptional point. *Nanophotonics* **10**, 403–423 (2021).
45. San-Jose, P., Cayao, J., Prada, E. & Aguado, R. Majorana bound states from exceptional points in non-topological superconductors. *Sci. Rep.* **6**, 1–13 (2016).
46. Kitaev, A. Y. Unpaired majorana fermions in quantum wires. *Physics-Uspekhi* **44**, 131 (2001).
47. Rahul, S., Kumar, R. R., Kartik, Y. & Sarkar, S. Majorana zero modes and bulk-boundary correspondence at quantum criticality. *J. Phys. Soc. Jpn.* **90**, 094706 (2021).
48. Kumar, R. R., Kartik, Y., Rahul, S. & Sarkar, S. Multi-critical topological transition at quantum criticality. *Sci. Rep.* **11**, 1–20 (2021).
49. Niu, Y. *et al.* Majorana zero modes in a quantum ising chain with longer-ranged interactions. *Phys. Rev. B* **85**, 035110 (2012).
50. Sarkar, S. Quantization of geometric phase with integer and fractional topological characterization in a quantum ising chain with long-range interaction. *Sci. Rep.* **8**, 5864 (2018).
51. Kartik, Y. R., Kumar, R. R., Rahul, S., Roy, N. & Sarkar, S. Topological quantum phase transitions and criticality in a longer-range kitaev chain. *Phys. Rev. B* **104**, 075113. https://doi.org/10.1103/PhysRevB.104.075113 (2021).
52. Anderson, P. W. Coherent excited states in the theory of superconductivity: Gauge invariance and the meissner effect. *Phys. Rev.* **110**, 827 (1958).
53. Sarkar, S. A study of quantum berezinskii-kosterlitz-thouless transition for parity-time symmetric quantum criticality. *Sci. Rep.* **11**, 1–12 (2021).
54. Verresen, R., Jones, N. G. & Pollmann, F. Topology and edge modes in quantum critical chains. *Phys. Rev. Lett.* **120**, 057001 (2018).
55. Berry, M. V. Physics of nonhermitian degeneracies. *Czechoslovak J. Phys.* **54**, 1039–1047 (2004).

56. Hasan, M. Z. & Kane, C. L. Colloquium: topological insulators. *Rev. Mod. Phys.* **82**, 3045 (2010).
57. Lee, T. E. Anomalous edge state in a non-hermitian lattice. *Phys. Rev. Lett.* **116**, 133903 (2016).
58. Xiong, Y. Why does bulk boundary correspondence fail in some non-hermitian topological models. *J. Phys. Commun.* **2**, 035043. https://doi.org/10.1088/2399-6528/aab64a (2018).
59. Zirnstein, H.-G., Refael, G. & Rosenow, B. Bulk-boundary correspondence for non-hermitian hamiltonians via green functions. *Phys. Rev. Lett.* **126**, 216407. https://doi.org/10.1103/PhysRevLett.126.216407 (2021).
60. Guo, G.-F., Bao, X.-X. & Tan, L. Non-hermitian bulk-boundary correspondence and singular behaviors of generalized brillouin zone. *New J. Phys.* **23**, 123007. https://doi.org/10.1088/1367-2630/ac38ce (2021).
61. Xiao, L. *et al.* Non-hermitian bulk-boundary correspondence in quantum dynamics. *Nature Phys.* **16**, 761–766 (2020).
62. Helbig, T. *et al.* Generalized bulk-boundary correspondence in non-hermitian topolectrical circuits. *Nature Phys.* **16**, 747–750 (2020).

Acknowledgements

The authors would like to acknowledge DST (EMR/2017/000898 and CRG/2021/000996) and AMEF for the funding and RRI library for the books and journals. Authors would like to thank Mr. Ranjith R Kumar and Y R Kartik for useful discussion. Finally authors would like to acknowledge ICTS Lectures/seminars/workshops/conferences/discussion meetings of different aspects in physics and virtual PHHQP seminar series.

Author contributions

S.S. identified the problem, S.R. solved the problem and wrote the manuscript under the guidence of S.S. Both authors analyzed the results and reviewed the manuscript.

Competing interests

The authors declare no competing interests.

Additional information

Correspondence and requests for materials should be addressed to S.S.

Reprints and permissions information is available at www.nature.com/reprints.

Publisher's note Springer Nature remains neutral with regard to jurisdictional claims in published maps and institutional affiliations.